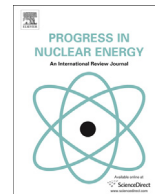




Contents lists available at ScienceDirect

Progress in Nuclear Energy

journal homepage: www.elsevier.com/locate/pnucene

Comparison of two three-dimensional heterogeneous Variational Nodal Methods for PWR control rod cusping effect and pin-by-pin calculation

Yongping Wang, Hongchun Wu, Yunzhao Li*

School of Nuclear Science and Technology, Xi'an Jiaotong University, 28 West Xianning Road, Xi'an, Shaanxi 710049, China

ARTICLE INFO

Article history:

Received 11 September 2016

Received in revised form

9 December 2016

Accepted 1 June 2017

Available online xxx

Keywords:

Variational Nodal Method

Heterogeneous

Pin-by-pin

Control rod cusping effect

ABSTRACT

Two heterogeneous nodal methods based on the Variational Nodal Method (VNM) are investigated with diffusion approximation in three-dimensional Cartesian geometry. The first one is named as Function Expansion (FE) method while the second is Finite Sub-element (FS) method. Based on our previous work and the code Violet-Het1D in one-dimensional slab geometry, a code named Violet-Het3D was developed to handle the Pressurized Water Reactor (PWR) control rod cusping effect and pin-by-pin calculation by using either of these two methods. To eliminate the control rod cusping effect, Violet-Het3D provides a different idea from the existing methods. Neither homogenization procedure nor mesh adjustment is needed in Violet-Het3D by taking advantage of the treatment for heterogeneous nodes. Numerical results show that both the FE and FS methods can eliminate the cusping effect and obtain accurate power distribution while the FE method has relatively higher efficiency and accuracy. In contrast, for pin-by-pin calculation, the FS method obtains more accurate eigenvalue and pin power distribution than the FE method.

© 2017 Published by Elsevier Ltd.

1. Introduction

In recent decades, the two-step scheme (Smith, 1986) is employed in Pressurized Water Reactor (PWR) core computation: lattice calculation with homogenization and whole-core diffusion calculation with pin-power reconstruction. For the core diffusion calculation, nodal methods have been widely employed. In nodal methods, there is one basic assumption that the cross sections within each node are homogeneous. Although the assumption is reasonable in most situations in PWR as the detailed construction within each assembly is homogenized by using the lattice code, it will introduce errors or limit the computational efficiency in some special cases. Two typical examples including the “control rod cusping effect” and pin-by-pin calculation are discussed in this paper.

Firstly, control rods keep moving along the axial direction within the PWR core with a step size of about 1–2 cm, while the nodal size of neutronics simulation is usually about 10–20 cm. Thus, unavoidably a control rod assembly may be partially inserted

into a node which means part of the node uses assembly-homogenized cross sections with control rods in while the other part uses assembly-homogenized cross sections with control rods out. As the piece-wise distributed cross sections within a node is not allowed by traditional nodal methods, the heterogeneous node should be homogenized. However, if we simply homogenize the node by using the volume-weighted scheme, it would result a lot of wiggles in the numerically simulated curve of control rod differential worth which theoretically should be smooth. This phenomenon is the so-called control rod cusping effect (Si, 2006). Since 1980s (Han-Sem, 1984), many methods have been investigated to eliminate it. These methods can be classified into two categories although they have different implementations. The first category is flux-volume-weighted methods (Yamamoto, 2004; Dall'Osso, 2002; Bandini et al., 2003; Downar et al., 2004; Reitsma and Muller, 2002). They have to obtain an approximate flux distribution over the heterogeneous nodes for homogenization. The second category is adaptive mesh methods (Zhang, 2014). They adjust the spatial mesh after each control rod movement to avoid the

* Corresponding author.

E-mail address: yunzhao@mail.xjtu.edu.cn (Y. Li).

appearance of heterogeneous nodes.

Secondly, to reduce the error introduced by assembly homogenization, the pin-by-pin scheme has arisen. It solves the whole-core problem with pin cell homogenized cross sections to eliminate the assembly homogenization and pin-power reconstruction. Therefore, many pin-by-pin calculation codes have been developed such as SCOPE2 (Tatsumi and Yamamoto, 2003) and EFEN (Li et al., 2014a). However, as traditional nodal method requires homogenized cross sections in each mesh, the whole-core pin-by-pin problem should consist of millions of meshes, causing issues in both memory and efficiency. For example, a PWR can be divided into 10 million pin-size meshes. Together with the SP₃ approximation and 4 energy groups, it needs 10 GB memory and the computational time is about 24 h (Yang et al., 2014) for one single CPU.

For the control rod cusping effect problem, if nodal method allows heterogeneity in a node, neither the flux-volume-weighted method nor the mesh adjustment would be needed to avoid the heterogeneous nodes. The control rod cusping effect is supposed to be directly eliminated by using heterogeneous nodal method. For the pin-by-pin problem, a whole assembly can be treated as a node if heterogeneity is allowed in a node.

Thus, to eliminate the requirement of nodal homogeneous cross sections in traditional nodal methods, heterogeneous nodal methods were developed. In 1997, Fanning and Palmiotti (1997) developed a heterogeneous Variational Nodal Method (VNM (Palmiotti et al., 1995; Li et al., 2015a)). The space variable of flux and current in this method are still expanded by polynomials as same as that in homogeneous VNM. For calculating the response matrices, the heterogeneous node is divided into several homogeneous regions and then the integrals over the node are divided into a set of homogeneous integrals. In 2003, Smith et al. (2003) developed another heterogeneous VNM. The main idea of this method is to further break each heterogeneous node into sub-elements within which the cross sections are constants. The flux is then expanded by finite trial functions in space. The nodal functional is constructed by the functional of all sub-elements in the node.

To investigate and make comparisons of the above two methods, this paper derives the formulations based on the two methods with diffusion approximation in three-dimensional Cartesian geometry. In this paper, we call them the function expansion (FE) method (Li et al., 2014b) and finite sub-element (FS) (Li et al., 2015b) method respectively. However, different from Fanning's method, the cross sections in FE method are presented by piecewise polynomials which means it can treat not only the problems with heterogeneous nodes consisted of several homogeneous regions as that in Fanning's paper, but also the problems with continuous cross sections (Li et al., 2014b) within the nodes. Different from Smith's method, the nodal interface current in FS method is expanded by finite trial functions instead of polynomials which should eliminate the interface approximation caused by the transformation of coefficients between finite trial functions and polynomials. Moreover, this paper applies these two methods to eliminating the control rod cusping effect in PWR which is not found in previous works. This might be the first practical application of heterogeneous nodal methods.

A commercial program called Freefem++ (Bernardi et al.,) is employed to generate the sub-elements inside the nodes. A code named Violet-Het3D was developed to treat heterogeneous node by the two methods. In addition, a representative PWR control rod cusping effect problem and a pin-by-pin problem were employed in this paper to make the comparisons for these two methods.

2. Theory

Both of the FE and FS methods start from the three-dimensional within-group diffusion equation:

$$\begin{cases} \nabla \cdot \mathbf{J}(\mathbf{r}) + \Sigma_t(\mathbf{r})\Phi(\mathbf{r}) = \Sigma_s(\mathbf{r})\Phi(\mathbf{r}) + S(\mathbf{r}) \\ \frac{1}{3}\nabla\Phi(\mathbf{r}) + \Sigma_t(\mathbf{r})\mathbf{J}(\mathbf{r}) = 0 \end{cases} \quad (1)$$

where Φ is the scalar flux ($\text{cm}^{-2} \cdot \text{s}^{-1}$), \mathbf{J} is net current ($\text{cm}^{-2} \cdot \text{s}^{-1}$), Σ_t is the total cross section (cm^{-1}), Σ_s is the within-group scattering cross section (cm^{-1}), and S is the source term ($\text{cm}^{-3} \cdot \text{s}^{-1}$) including scattering and fission:

$$S(\mathbf{r}) = \sum (\mathbf{r})\Phi(\mathbf{r}) + \frac{1}{k}Q(\mathbf{r})\Phi(\mathbf{r}) \quad (2)$$

where

$$\sum (\mathbf{r})\Phi(\mathbf{r}) = \sum_{g' \neq g} \Sigma_{gg'}^s(\mathbf{r})\Phi_{g'}(\mathbf{r}) \quad (3)$$

and

$$\frac{1}{k}Q(\mathbf{r})\Phi(\mathbf{r}) = \sum_g \frac{\chi_g}{k} \nu \Sigma_{fg}(\mathbf{r})\Phi_g(\mathbf{r}) \quad (4)$$

k is the effective multiplication factor, $\chi_g \nu \Sigma_{fg}$ and $\Sigma_{gg'}$ are respectively the fission and scattering cross sections (cm^{-1}) from energy group g' to g .

The same as the homogeneous VNM, the entire problem domain is decomposed into subdomains V_v (nodes) and the functional can be written as a superposition of nodal contributions:

$$F[\Phi, J] = \sum_v F_v[\Phi, J] \quad (5)$$

$F[\Phi, J]$ stands for the functional of the whole problem in terms of Φ and J while $F_v[\Phi, J]$ is the nodal functional. Start from here, the FE and FS methods treat the nodal heterogeneity differently.

2.1. Function expansion method

The nodal functional consists of volume and surface contributions:

$$F_v[\Phi, J] = \int_v dV \left\{ \frac{1}{3} \Sigma_t(\mathbf{r})^{-1} (\nabla\Phi(\mathbf{r}))^2 + (\Sigma_t(\mathbf{r}) - \Sigma_s(\mathbf{r}))\Phi(\mathbf{r})^2 - 2\Phi(\mathbf{r})S(\mathbf{r}) \right\} + 2 \sum_\gamma \int_\gamma \Phi_\gamma J_\gamma d\Gamma \quad (6)$$

$$J_\gamma = \mathbf{J}_\gamma \cdot \mathbf{n}_\gamma \quad (7)$$

where v stands for a certain node of the entire problem; γ represents a certain nodal surface of node v ; J_γ stands for the net current ($\text{cm}^{-2} \cdot \text{s}^{-1}$) on the surfaces of the node and \mathbf{n}_γ is the outer normal of the nodal surface. In this method, the cross sections in the nodal functional as shown in Eq. (6) can be written as piecewise polynomials instead of constants. Thus, it can treat both the problems of heterogeneous nodes with piecewise homogeneous regions and the problems with continuous cross sections.

Then the scalar flux, the within-group source within the nodes and net current along the nodal surfaces are expanded as:

$$\begin{cases} \Phi(\mathbf{r}) = \sum_i \varphi_i f_i(\mathbf{r}) \\ S(\mathbf{r}) = \sum_i s_i f_i(\mathbf{r}) \\ J_\gamma(\mathbf{r}) = \sum_j \chi_{j\gamma} h_j(\mathbf{r}) \end{cases} \quad (8)$$

where $f(\mathbf{r})$ and $h(\mathbf{r})$ are the known orthogonal polynomials defined in the volume and on the surfaces respectively; φ_i, s_i and $\chi_{j\gamma}$ are the corresponding unknown coefficients or expansion moments. Substituting Eq. (8) into Eq. (2), we can obtain the relationship between flux and source moments:

$$s_i = \int_v \left\{ \left(\Sigma(\mathbf{r}) + \frac{1}{k} Q(\mathbf{r}) \right) \cdot \left(\sum_i \varphi_i f_i(\mathbf{r}) \right) \cdot f_i(\mathbf{r}) \right\} \quad (9)$$

Inserting Eq. (8) into Eq. (6) yields the reduced functional for each node:

$$F_v[\varphi, \chi] = \varphi^T \mathbf{A} \varphi - 2\varphi^T \mathbf{s} + 2\varphi^T \mathbf{M} \chi \quad (10)$$

$$\mathbf{M} = [\mathbf{M}_1, \mathbf{M}_2, \dots, \mathbf{M}_\gamma, \dots] \quad (11)$$

$$\chi^T = [\chi_1^T, \chi_2^T, \dots, \chi_\gamma^T, \dots] \quad (12)$$

where

$$A_{i'i'} = \int_v \{ D(\mathbf{r}) \cdot \nabla f_i(\mathbf{r}) \cdot \nabla f_{i'}(\mathbf{r}) + (\Sigma_t(\mathbf{r}) - \Sigma_s(\mathbf{r})) f_i(\mathbf{r}) \cdot f_{i'}(\mathbf{r}) \} dV \quad (13)$$

$$D(\mathbf{r}) = \frac{1}{3} \Sigma_t(\mathbf{r})^{-1} \quad (14)$$

$$M_{ij\gamma} = \int_\gamma f_i(\mathbf{r}) h_j(\mathbf{r}) d\Gamma \quad (15)$$

φ, \mathbf{s} and χ are the unknown vectors consisted of φ_i, s_i and $\chi_{j\gamma}$.

Different from the homogeneous VNM, the cross sections in Eqs. (9) and (13) cannot be taken out of the integration. Once the nodal functional is obtained, the following derivation is the same as that in homogeneous VNM. This method directly describes the cross section as a function of space through the derivation and finally considers the nodal heterogeneity into the integrals of response matrix \mathbf{A} .

2.2. Finite sub-element method

In this method, each node is further divided into a set of homogeneous sub-regions named sub-elements (Smith et al., 2003). The nodal functional is then written as a superposition of sub-element functional:

$$F_v[\Phi, J] = \sum_e F_e[\Phi_e, J] \quad (16)$$

where e stands for a certain element in the nodal domain. Then the element functional is written as:

$$\begin{aligned} F_e[\Phi_e, J] = & \int_e dV \left\{ D_e (\nabla \Phi_e)^2 + (\Sigma_{t,e} - \Sigma_{s,e}) \Phi_e^2 - 2\Phi_e S_e \right\} + 2 \sum_\gamma \\ & \times \int_\gamma \Phi_{e,\gamma} J_{e,\gamma} d\Gamma \end{aligned} \quad (17)$$

The surface term in Eq. (17) only appears in those sub-elements adjacent to nodal interfaces because continuous trial functions are used within each node.

We expand the flux and source within the sub-element and net current along the sub-element's surfaces as:

$$\begin{cases} \Phi_e(\mathbf{r}) = \sum_{m=1}^M \varphi_{e,m} f_{e,m}(\mathbf{r}) \\ S_e(\mathbf{r}) = \sum_{m=1}^M s_{e,m} f_{e,m}(\mathbf{r}) \\ J_{e,\gamma}(\mathbf{r}) = \sum_{n=1}^N j_{e,\gamma,n} h_{e,\gamma,n}(\mathbf{r}) \end{cases}, \mathbf{r} \in e \quad (18)$$

Different from polynomial expansions in FE method, $f(\mathbf{r})$ and $h(\mathbf{r})$ are the linear finite element trial functions (Zienkiewicz et al., 2008) defined in the volume and on the surfaces. φ, \mathbf{s} and \mathbf{j} are the unknown coefficients. M and N respectively represent the number of vertices within the sub-element and on its surface. For the cross sections in each element are homogeneous, the relationship between flux and source moments is written as:

$$s_{e,m} = \left(\Sigma_e + \frac{1}{k} \nu \Sigma_{f,e} \right) \varphi_{e,m} \quad (19)$$

Substituting Eq. (18) into the element functional in Eq. (17) yields the reduced functional:

$$F_e[\varphi, \mathbf{j}] = \varphi_e^T \mathbf{A}_e \varphi_e - 2\varphi_e^T \mathbf{F}_e \mathbf{s}_e + 2\varphi_e^T \mathbf{M}_e \mathbf{j}_e \quad (20)$$

where

$$\begin{aligned} A_{e,mm'} = & \int_e \left\{ D_e \cdot \nabla f(\mathbf{r})_{e,m} \cdot \nabla f_{e,m'}(\mathbf{r}) + (\Sigma_{t,e} \right. \\ & \left. - \Sigma_{s,e}) f_{e,m}(\mathbf{r}) f_{e,m'}(\mathbf{r}) \right\} dV \end{aligned} \quad (21)$$

$$F_{e,mm'} = \int_e f_{e,m}(\mathbf{r}) f_{e,m'}(\mathbf{r}) dV \quad (22)$$

$$M_{e,mn'} = \int_\gamma f_{e,m}(\mathbf{r}) h_{e,\gamma,n'}(\mathbf{r}) d\Gamma \quad (23)$$

To obtain the nodal functional, we should use the Boolean transformation matrix (Reddy, 1993) Ξ_e to map the element trial function coefficients to the nodal expansion coefficients:

$$\varphi_e = \Xi_e \varphi \quad (24)$$

Substituting Eq. (24) into Eq. (20), and then substituting Eq. (20) into Eq. (16) leads to the nodal functional:

$$F_v[\varphi, \mathbf{j}] = \varphi^T \mathbf{A} \varphi - 2\varphi^T \mathbf{s} + 2\varphi^T \mathbf{M} \mathbf{j} \quad (25)$$

where

$$\mathbf{A} = \sum_e \Xi_e^T \mathbf{A}_e \Xi_e \quad (26)$$

$$\mathbf{s} = \sum_e \Xi_e^T \mathbf{F}_e \mathbf{s}_e \quad (27)$$

$$\mathbf{M} = [\Xi_1^T \mathbf{M}_1 \quad \Xi_2^T \mathbf{M}_2 \quad \dots \quad \Xi_e^T \mathbf{M}_e \quad \dots] \quad (28)$$

$$\mathbf{j}^T = [\mathbf{j}_1^T \quad \mathbf{j}_2^T \quad \dots \quad \mathbf{j}_e^T \quad \dots] \quad (29)$$

Then we can obtain the nodal response equations by the same procedure in homogeneous VNM.

3. Results

A typical PWR control rod cusping effect problem and a pin-by-pin problem were calculated to test the ability of the code Violet-Het3D for treating heterogeneous nodes. All the following comparisons take homogeneous fine mesh calculation as the reference because it can directly measure the error introduced by the treatments of heterogeneity in FE and FS method. Therefore, another code Violet-Hom3D (Li et al., 2015a), based on homogeneous VNM, is developed.

3.1. Control rod cusping effect

The configuration of the 1/4 core is shown in Figs. 1 and 2. “CR” represents the assemblies with control rods and the radial size of all the assemblies is 20 × 20 cm. The two-group macroscopic cross sections of assemblies and reflector are listed in Table 1.

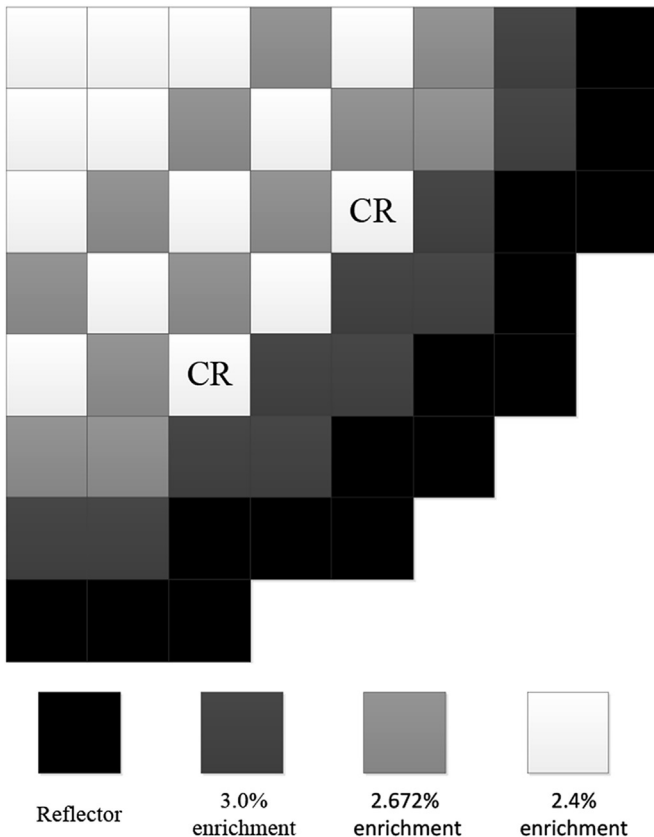


Fig. 1. Radial configuration of the 1/4 reactor core.

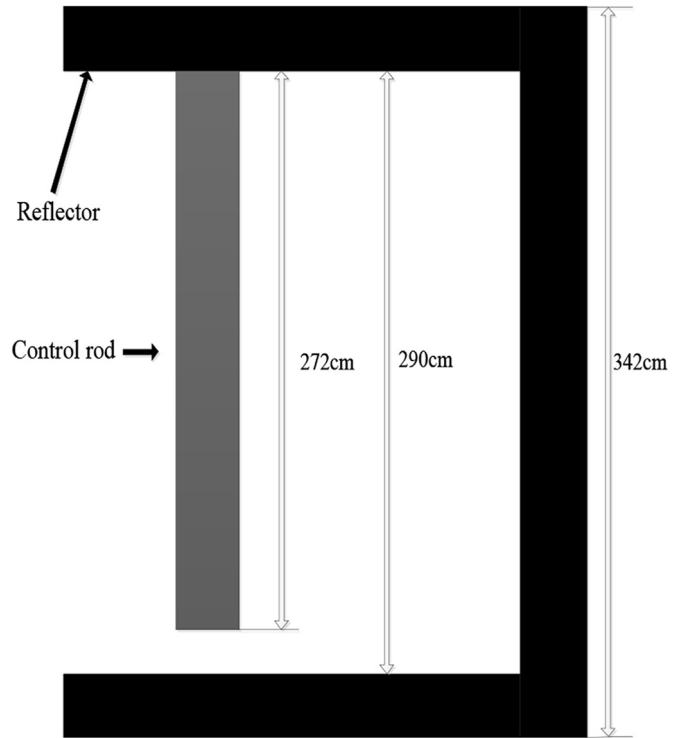


Fig. 2. Axial size of the reactor core.

In this problem, the control rods were inserted from the top to the bottom of the core by 1 cm for each step. Fig. 2 shows that there are totally 272 steps. Then the differential worth of the control rods can be calculated by the eigenvalues obtained by the whole-core diffusion calculation for each step. For example, the control rods differential worth of step *i* (from top to bottom) can be calculated by:

$$Diff_i = \left(\frac{k_i - 1}{k_i} - \frac{k_{i-1} - 1}{k_{i-1}} \right) * 10^5 \text{ pcm/cm}, i = 1, \dots, 272 \quad (30)$$

where *k_i* and *k_{i-1}* are the eigenvalues obtained by the whole-core diffusion calculations for step *i* and *i-1* respectively of the control rods.

To obtain the reference control rod differential worth, we divide each assembly into 4 nodes in radial and take 1 cm for the axial size. So the size of each node is 10 × 10 × 1 cm. Heterogeneous nodes will not exist in this situation as fine nodal mesh is adopted in the axial direction. Violet-Hom3D is employed for the reference calculation.

Actually, in the core-analysis calculation, nodal size is usually about 10–20 cm in axial direction. In this problem, as indicated by Fig. 2, the axial size of the nodes should be 26 cm in the reflector region and 20 cm in the core except a layer of 10 cm at the bottom of the core. In this situation, heterogeneous nodes will appear with the movement of the control rod as is shown in Fig. 3. To obtain the homogenous cross sections of the heterogeneous nodes, the easiest method is volume-weighted scheme. However, this scheme causes severe control rod cusping effect as is shown in Fig. 4. A more commonly used method is flux-volume-weighted scheme. Then the homogeneous cross sections of the heterogeneous nodes are obtained by:

Table 1
Two-group macroscopic cross sections of different materials.

Material	Energy group	D_g/cm	$\Sigma_{a,g}/cm^{-1}$	$\nu\Sigma_{f,g}/cm^{-1}$	$\Sigma_{s,1-2}/cm^{-1}$
Fuel assembly (3.0% enrichment)	1	1.4191287	0.0087124	0.0061720	0.0167086
	2	0.3743527	0.0799658	0.1203360	
Fuel assembly (2.672% enrichment)	1	1.4166403	0.0085210	0.0057686	0.0169843
	2	0.3744220	0.0751517	0.1103079	
Fuel assembly (2.4% enrichment)	1	1.4143051	0.0083632	0.0054297	0.0172346
	2	0.3744912	0.0703376	0.0997627	
CR	1	1.4317809	0.0120676	0.0053785	0.0147629
	2	0.3793716	0.0940192	0.1026720	
Reflector at the top	1	1.5552857	0.0076996	0.0	0.0210846
	2	0.3616395	0.1385250	0.0	
Reflector at the bottom	1	1.2762708	0.0016599	0.0	0.0326260
	2	0.2824586	0.0397660	0.0	
Reflector around	1	1.1322748	0.0027034	0.0	0.0210846
	2	0.2489262	0.0193220	0.0	

$\chi_1 = 1.0, \chi = 0.0$

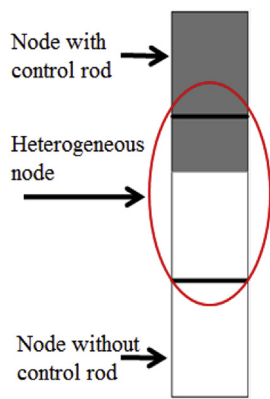


Fig. 3. Heterogeneous node caused by control rod.

$$\Sigma_{Hom} = \frac{\int_{HetNode} \Sigma_{Het}(z)\varphi(z)dz}{\int \varphi(z)dz} \quad (31)$$

To obtain the axial flux distribution for homogenization in Eq. (31), it has to iterate between the one-dimensional calculation of the assembly with control rod in the axial direction and the three-dimensional calculation of the core. The 3D dimensional calculation aims to provide radial leakage for the 1D calculation. Then the 1D calculation obtains the axial flux distribution and homogenizes the cross sections for the 3D calculation. The iteration should do at least once to obtain acceptable accuracy. The result of this scheme is also shown in Fig. 4. We can find that the cusping effect is greatly reduced but still exist. All the above calculations are done by Violet-Hom3D. Additionally, if we use axial discontinuity factor in the flux-volume-weighted scheme, the accuracy will be further

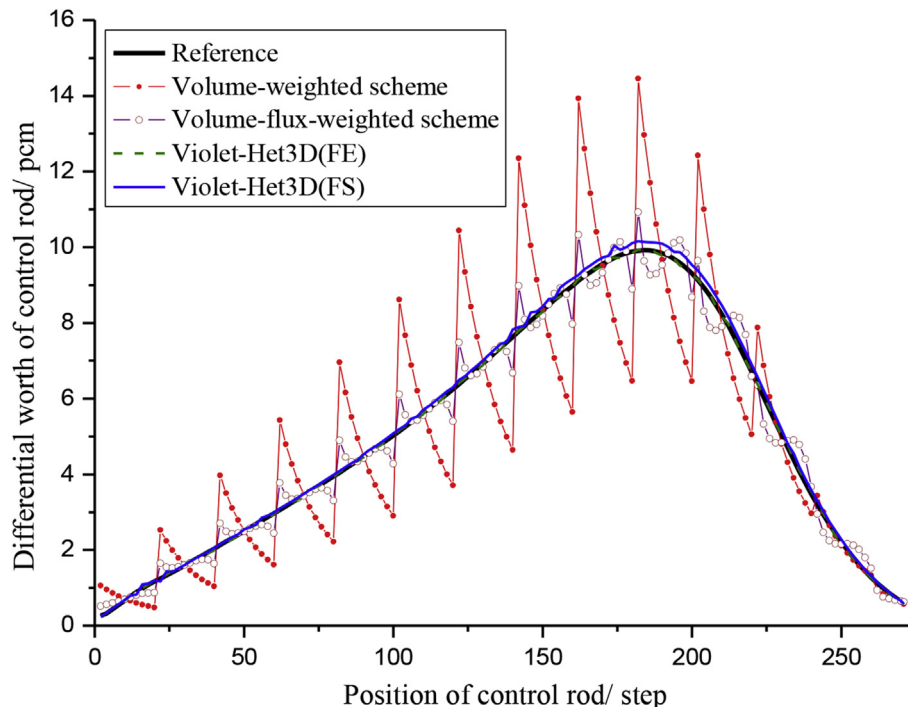


Fig. 4. Differential worth of control rod calculated by different scheme.

improved. However, to make consistent and fair comparisons, this paper didn't use any axial discontinuity factors in all the calculations.

Violet-Het3D adopts the same coarse mesh mentioned above, for heterogeneity is allowed in this method, homogenization is not needed for the nodes with control rod partially inserted. In FE method, the distributions of cross sections in the heterogeneous nodes are described as piecewise functions of space in Violet-Het3D:

$$\Sigma_{x,g}(\mathbf{r}) = \begin{cases} \Sigma_1, z \in [z_0, z_1] \\ \Sigma_2, z \in [z_1, z_2] \end{cases} \quad (32)$$

z_0 and z_2 represent the axial positions of the bottom and top of the heterogeneous node; z_1 is the cross section discontinuity position; Σ_1 and Σ_2 are the two different values of one kind of cross section within the heterogeneous node. In the FE method, the flux is expanded by 5th order polynomials in the axial direction. In contrast, the heterogeneous nodes are explicitly described by tetrahedrons in FS method. Each node is divided into 10 layers with 24 tetrahedrons for each layer. The numerical results of these two methods are also shown in Fig. 4. Obviously, Violet-Het3D obtains better results than flux-volume-weighted schemes. Both FE and FS methods can eliminate the cusping effect and provide a smooth differential worth curve which agrees well with the reference. While there is still some difference between the reference and the curve obtained by FS method especially at the top of the curve, it is due to the linear expansion approximation of the flux and source in the sub-element as indicated by Eq. (18). Increasing the number of sub-element in the nodes will improve the results.

This paper has also made the comparisons of power distributions when the control rods are at the 150th step in the core so that heterogeneous nodes appear in the middle of the core. Fig. 5 shows the relative percent error of the axial power distribution of the CR assembly obtained by different schemes. The relative percent error is defined by:

$$\text{error} = \frac{\text{result} - \text{reference}}{\text{reference}} * 100\% \quad (33)$$

We can find that the errors of volume-weighted scheme and volume-flux-weighted scheme locate in intervals -4% – 2% and -2% – 4% respectively. In addition, the maximum error exits around the heterogeneous node because homogenization procedure is applied in the two weighted schemes. In contrast, FE method and FS method achieve much better results with the maximum error less than 0.2% and 0.5% respectively.

Fig. 6 shows the relative percent error of the radial power distribution of the layer where heterogeneous node exits when volume-weighted scheme is applied. We can find the maximum error -3.5% – -4.3% occurs at the CR assembly. The large error of the CR assembly also affects the adjacent nodes with the maximum error of about -1.5% . The Root-Mean-Square (RMS) error of the distribution is 1.21%. The overall error decreases when we apply volume-flux-weighted scheme to this problem. The maximum error is 1.5% and it still exits at the CR assembly; the RMS error of the distribution is 0.42%. Although volume-flux-weighted scheme provides obvious improvement for the radial power distribution but the error is still too large. Fig. 7 shows the percent error of radial power distribution when FE method is employed in Violet-Het3D. The maximum error at the CR assembly is -0.02% and the errors of all other nodes are less than 0.01%. In addition, the RMS error is 0.01%. Obviously, the FE method has obtained much more accurate radial power distribution than the two weighted schemes. When FS method is adopted, the maximum error at the CR assembly becomes -0.05% and the errors of all other nodes are less than 0.03%. The RMS error is 0.02%. Comparatively, the FE method has relatively better accuracy than FS method in this problem.

Table 2 shows the computational time of different schemes. The reference calculation costs much more time than the others. The volume-weighted scheme costs the least time but suffers from severe cusping effect. As the flux-volume-weighted scheme has to do the iteration between 3D and 1D calculation at least once, the

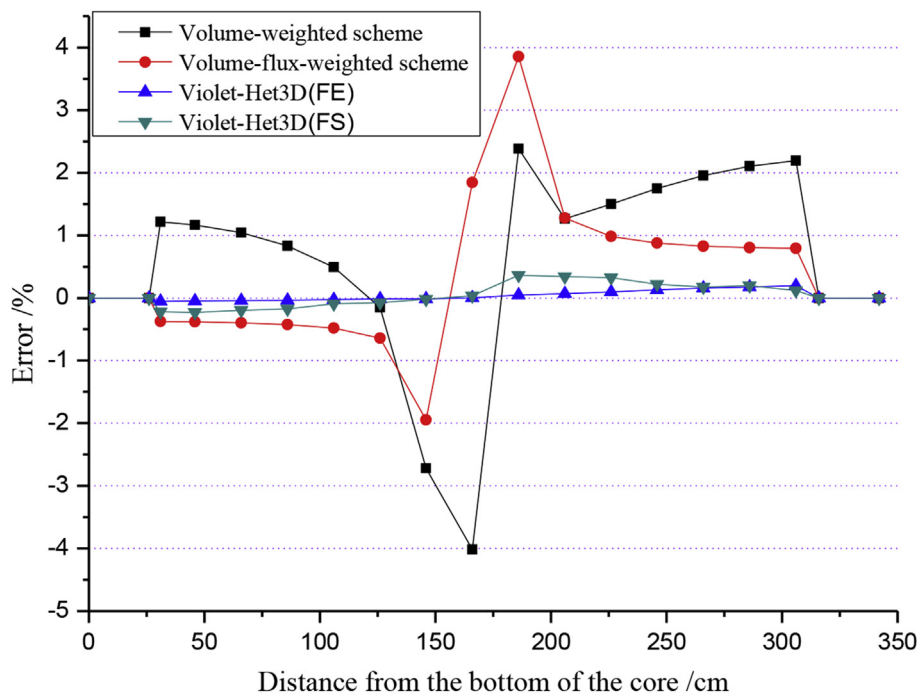


Fig. 5. Error of axial power distribution of the CR assembly.

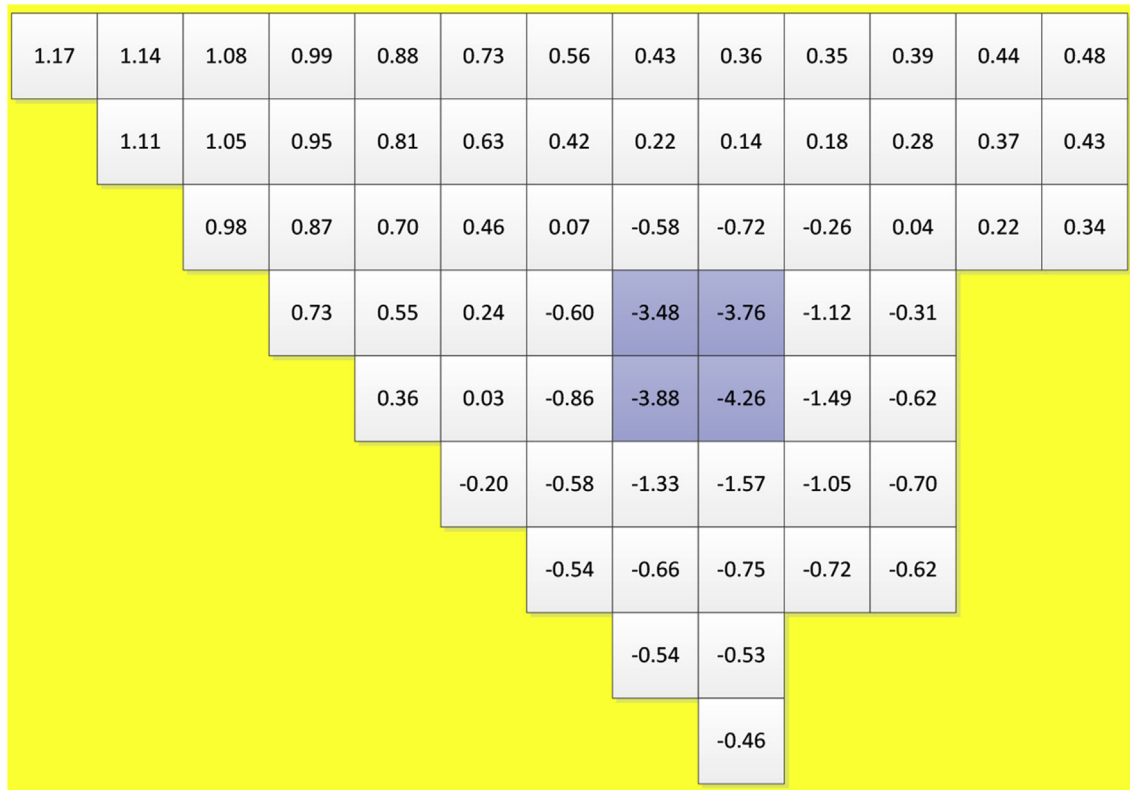


Fig. 6. Percent error of radial power distribution obtained by volume-weighted scheme.

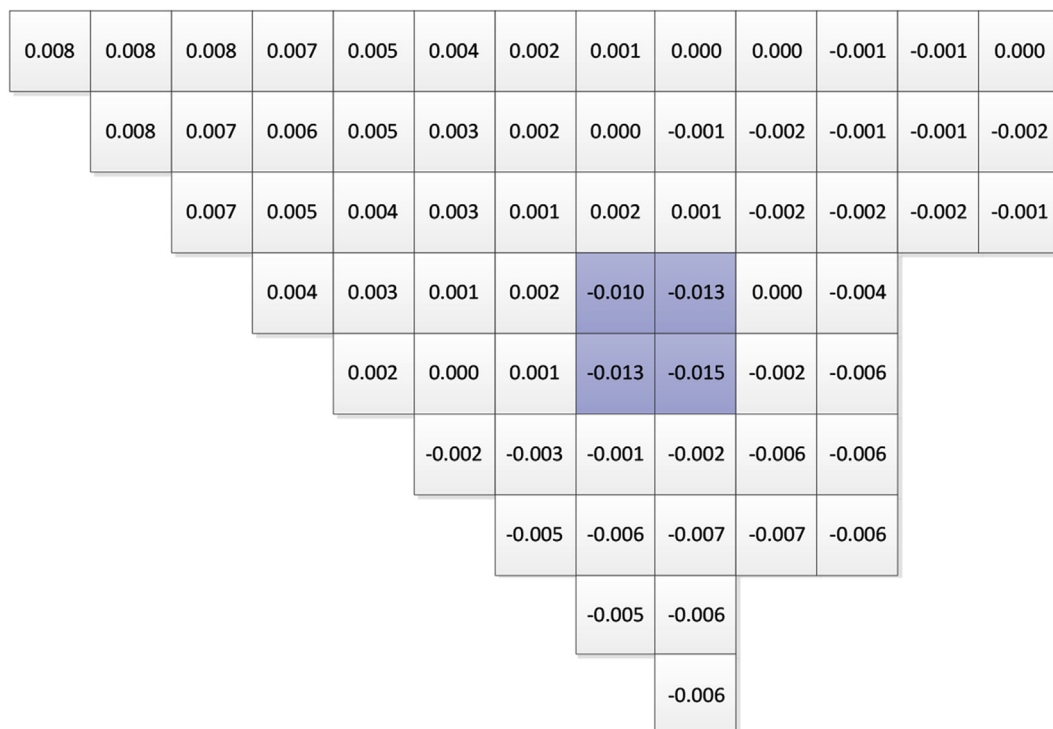


Fig. 7. Percent error of radial power distribution obtained by FE method in Violet-Het3D.

Table 2
Computational time of different schemes.

Schemes	Reference	Volume-weighted	Flux-volume-weighted	Violet-Het3D(FE)	Violet-Het3D(FS)
Time/min	>1000	141.5	331.7	155.3	196.0

computational time is more than twice as much as that of volume-weighted scheme. As indicated in Table 2, Violet-Het3D costs much less time than the flux-volume-weighted scheme. It is because no 3D-1D iteration for the homogenized cross sections is performed in Violet-Het3D. In addition, FE method shows higher efficiency in this problem than FS method. FE method costs 10% more time than the volume-weighted scheme while 40% for FS method. This is because 99 vertices and 240 tetrahedrons are defined within each node in Violet-Het3D to describe the movement of control rods which makes the response matrices get larger than those in FE method. Larger response matrices slow down the power iteration of Violet-Het3D.

3.2. Pin-by-pin problem

The radial core configuration of the problem is shown in Fig. 8. The size of each assembly is 21.46×21.46 cm. Each fuel assembly has traditional 17×17 pin configuration. Table 3 shows the two-group homogenized cross sections of different pin cells. Ideally the neutron-transport equation or at least the SP_3 equation should be solved in this problem. However, in order to evaluate Violet-Het3D's ability of treating spatial heterogeneity, the neutron-diffusion equation was solved for demonstration purpose.

The reference calculation treats each individual pin as a node

(including reflector assembly) making 2601 nodes in total. The same as before, Violet-Hom3D is employed in the reference calculation. In contrast, Violet-Het3D treats the entire assembly as a single node with heterogeneous structure inside. The number of nodes is only 9 for Violet-Het3D. As shown in Fig. 9, each assembly is divided into tetrahedrons by the commercial program called Freefem++ when FS method is adopted. And it can be found in Fig. 9 that each pin consists of 6 tetrahedrons which is enough to describe explicitly the heterogeneous assembly. Further increasing the number of tetrahedrons in the pin cell gains little improvement as the pin cell is homogenized.

The results of k_{eff} are shown in Table 4. As we can see, FS method achieves very accurate eigenvalue. In FE method, the error of k_{eff} decreases with the increase of expansion orders. However, little improvement has been obtained by further increasing the expansion order higher than 7 in the volume and 3 on the surface.

The comparison of power distribution is shown in Table 5. It can be found that the FS method provides more accurate power distribution than FE method. In FS method, the RMS error is 0.35% which is smaller than that in FE method. Moreover, 88% of the pin power errors are smaller than 0.5% and only 1.7% of them are larger than 1%. Additionally, an error of 0.08% for the maximum pin power is one order of magnitude smaller than that in FE method. Comparatively, in FE method, the results improve with the increase

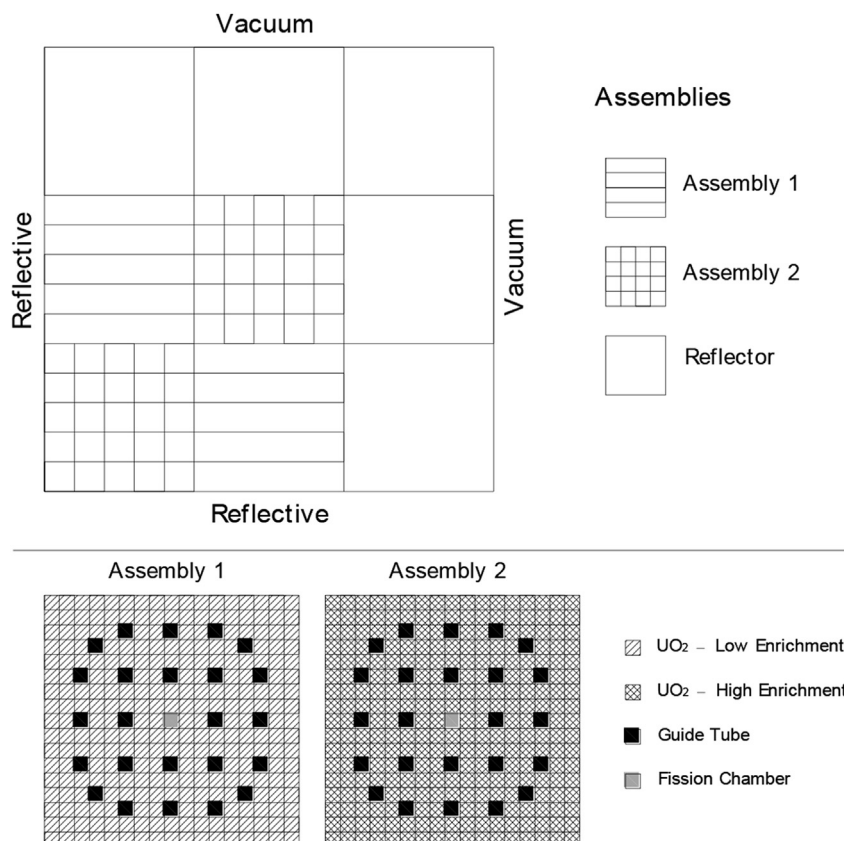


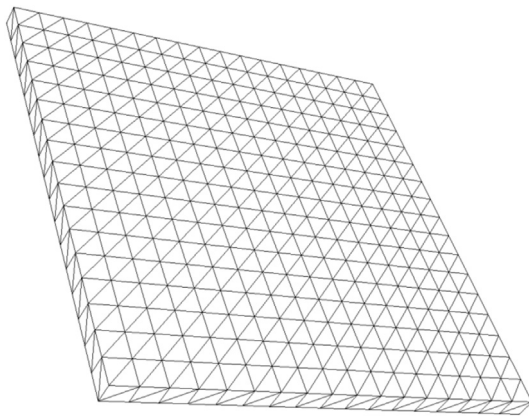
Fig. 8. Radial core and assembly configuration.

Table 3

Two-group macroscopic cross sections of the pin-by-pin problem.

Material	Energy group	D_g/cm	$\Sigma_{a,g}/cm^{-1}$	$\nu\Sigma_{f,g}/cm^{-1}$	$\Sigma_{s,1-2}/cm^{-1}$
Low Enrichment UO ₂	1	1.5445113	0.0087645	0.0048365	0.0163555
	2	0.4836491	0.0472279	0.0706837	
High Enrichment UO ₂	1	1.5532413	0.0094252	0.0056983	0.0173998
	2	0.4555234	0.0619177	0.0998909	
Guide Tube	1	1.9070722	0.0004357	0.0	0.0286373
	2	0.3934771	0.0070638	0.0	
Fission Chamber	1	1.9132458	0.0004154	0.0	0.0285656
	2	0.3925138	0.0070833	0.0	
Reflector	1	0.9055953	0.0029478	0.0	0.0268502
	2	0.3135986	0.1000718	0.0	

$\chi_1 = 1.0, \chi_0 = 0.0$

**Fig. 9.** Sub-elements configuration in each layer of the assembly.**Table 4** k_{eff} Comparison for the pin-by-pin problem when take each assembly as one node.

Reference	Violet-Het3D (FE)		Results Error/pcm	Violet-Het3D(FS)	Error/pcm
	Expansion				
	Volume	Surface			
1.10468	5	1	1.10527	59	1.10474
	7	1	1.10519	51	
	7	3	1.10504	36	
	9	3	1.10503	35	
	11	5	1.10499	31	

Table 5

Power Comparison of the pin-by-pin problem when take each assembly as one node.

Scheme	Expansion		Error of max. pin power/%	Max. error of pin power/%	No. of pins with different errors			RMS/%
	Volume	Surface			>1.0%	0.5–1.0%	<0.5%	
Violet-Het3D (FE)	5	1	2.58	4.63	268	326	462	1.10
	7	1	0.80	2.20	203	361	492	0.81
	7	3	0.78	1.54	98	409	549	0.60
	9	3	0.74	2.16	87	482	487	0.62
	11	5	0.57	1.80	78	356	622	0.55
Violet-Het3D (FS)	/	/	0.08	1.49	18	110	928	0.35

of expansion orders. However, the improvement is not obvious when we further increase the expansion order higher than 7 in the volume and 3 on the surface. The RMS error and the error of the maximum pin power are 0.55% and 0.57 respectively when the expansion order is as high as 11 in the volume and 5 on the surface. In addition, there are still 7% of the pin power errors exceeding 1% even with that high expansion order and most of them appear around the guide tube and fission chamber. As the strong discontinuity in cross sections (fuel, guide tube and fission chamber) causing sharp flux gradient and complicated flux distribution within the node, it's difficult for FE method to obtain accurate flux distribution when the flux is expanded by continuous polynomials over the entire assembly. Therefore, for FE method, most of the large errors exist around guide tube and fission chamber where the sharp flux gradient happens. By taking the advantage of element trial functions' capability of describing complicated flux distribution, FS method obtains more accurate pin power distribution within the assembly with the error less than 0.5%.

Table 6 shows the comparison of computational time. With the increase of expansion orders in FE method, the time for computing response matrices increases quickly while the time for iteration remains almost the same. Compared to the reference solution, the time for iteration in FE method decreases significantly because the number of nodes is only 9. However, to treat the heterogeneity in the node, more computational effort is needed by response matrix calculation as is shown in Eq. (13). For the FE method, the computational time for 9th order of volume expansion and 3rd order of surface expansion is 15.7s which is about two times more than that of the reference. FS method is supposed to be more efficient than the reference because it also decreases the number of nodes. However, as a result of the enormous number of vertices that had to be defined to model the complicate geometry of the assembly (648 vertices for each assembly in this problem), large response matrices are obtained. This will greatly increase not only the time of generating the response matrices, but also the time of iteration.

Additionally, we further divide the whole assembly into 4 nodes in Violet-Het3D calculations. So the assembly which contains

Table 6
Comparison of computational time of the pin-by-pin problem when take each assembly as one node.

Scheme	Expansion		Response matrices/s	Iterations/s	Total/s
	Volume	Surface			
Violet-Het3D(FE)	5	1	0.8	0.0	0.8
	7	1	3.8	0.0	3.8
	7	3	3.9	0.1	4.0
	9	3	15.6	0.1	15.7
	11	5	54.5	0.1	54.6
Violet-Het3D(FS)	/	5.5	4.0	9.5	
Reference	3	2	0.1	5.6	5.7

Table 7
 k_{eff} Comparison for the pin-by-pin problem when take each assembly as four nodes.

Reference	Violet-Het3D (FE)		Violet-Het3D(FS)		Error/pcm	
	Expansion		Results			
	Volume	Surface	Error/pcm			
1.10468	5	1	1.10548	80	1.10477	9
	7	1	1.10539	71		
	7	3	1.10510	42		
	9	3	1.10508	40		
	11	5	1.10492	24		

17 × 17 pin cells is broke up into 4 nodes containing 8 × 8, 8 × 9, 9 × 8 and 9 × 9 pin cells respectively. Each pin cell also consists of 6 tetrahedrons when FS method is employed. Tables 7 and 8 show the comparisons of eigenvalue and pin power. However, we can find the result of FE method doesn't become better than that shown in Tables 4 and 5, it even gets worse especially when the low expansion order is adopted on the surface. When the surface expansion order increases to 5th, the results are only slightly better than that of taking each assembly as a node. This is because when we divide the whole assembly into 4 nodes, there will be not only fuel pin cell, but also guide tube and fission chamber adjacent to nodal interfaces which causes complicated current distribution along the interface. The complex distribution should be difficult for low order polynomials to describe. In contrast, when we treat the whole assembly as one node, only fuel pin cells are adjacent to nodal interfaces as shown in Fig. 8. Thus, although the reduction of the number of pin cells in each node would improve the performance of FE method within the node, the interface approximation introduces in additional error in this case. Comparatively, the accuracy of FS method remains the level because there are 8 basis functions in each pin cell to represent the flux distribution and 4 basis functions on each pin cell surface which are capable of describing the current.

Table 9 shows the computational time when we take each assembly as 4 nodes. By comparing with Table 6, we can find the computational time for response matrices doesn't change much. It is because although fewer pin cells in each node reduces the

computational effort of generating response matrices for each node, the number of "unique nodes" (have different geometry or material configuration from any other nodes) increases in the whole problem. In the meanwhile, with the larger total number of nodes, the iteration time increases but it has relative small value. As a result, the total computational time is similar to that shown in Table 6.

4. Conclusions

This paper investigated two heterogeneous nodal method based on VNM with diffusion approximation in three-dimension Cartesian geometry. Correspondingly, a code named Violet-Het3D was developed. FE method directly considers the cross sections in each node as functions of space through the derivation and expands the flux over the entire node by continuous polynomials. In contrast, FS method further divides the heterogeneous node into homogeneous regions and expands the flux by linear trial functions. Two test problems, a PWR control rod cusping effect problem and a pin-by-pin problem, were calculated to test the treatments for heterogeneous node of the two methods.

To eliminate the control rod cusping effect, traditional methods usually adopt rehomogenization schemes or adjust the nodal mesh to avoid the appearance of heterogeneous nodes. In contrast, Violet-Het3D provides a new scheme. It directly treats the heterogeneous nodes without rehomogenization or mesh adjustment. Encouraging numerical results have been obtained. The volume-weighted scheme suffers from most severe cusping effect. The flux-volume-weighted scheme can reduce the cusping effect but cannot eliminate it. Both FE and FS methods in Violet-Het3D can obtain a very smooth differential worth curve which agrees well with the reference. Moreover, they can also achieve accurate axial and radial power distribution. In terms of efficiency, as FS method has to divide the finite elements in the nodes, it causes considerable increase in computational time compared with the volume-weighted scheme. However, FE method only cost about 10% more time than the volume-weight scheme while obtaining high accuracy. Thus, FE method is more recommended to be employed to handle the cusping effect. Additionally, FE method can be easily implemented in an existing VNM code.

Table 8
Power Comparison of the pin-by-pin problem when take each assembly as four nodes.

Scheme	Expansion		Error of max. pin power/%	Max. error of pin power/%	No. of pins with different errors			RMS/%
	Volume	Surface			>1.0%	0.5–1.0%	<0.5%	
Violet-Het3D (FE)	5	1	3.10	6.21	316	368	372	1.80
	7	1	1.60	3.50	242	390	424	0.98
	7	3	0.86	1.84	112	416	528	0.69
	9	3	0.79	2.00	90	464	502	0.62
	11	5	0.50	1.68	74	362	620	0.54
Violet-Het3D (FS)	/		0.07	1.80	18	116	922	0.36

Table 9

Comparison of computational time of the pin-by-pin problem when take each assembly as four nodes.

Scheme	Expansion		Response matrices/s	Iterations/s	Total/s
	Volume	Surface			
Violet-Het3D(FE)	5	1	0.7	0.0	0.7
	7	1	3.7	0.1	3.8
	7	3	3.9	0.3	4.2
	9	3	15.2	0.3	15.5
	11	5	51.8	0.5	52.3
Violet-Het3D(FS)	/	/	5.0	4.9	9.9
Reference	3	2	0.1	5.6	5.7

Numerical results of the pin-by-pin problem show that FS method obtains relatively better accuracy in eigenvalue and pin power distribution than FE method. With FS method, the error of eigenvalue is 6 pcm. The RMS error and the error of maximum pin power are 0.35% and 0.08% respectively. Moreover, nearly 90% of the pin power errors are less than 0.5%. With FE method, the RMS error and the error of the maximum pin power are 0.55% and 0.57 respectively even the expansion order is as high as 11 in the volume and 5 on the surface. In addition, as the complicated flux distribution over the entire assembly is expanded by continuous polynomials, 7% of the pin power errors exceed 1.0% which happens around the regions with cross sections discontinuity (such as the region close to guide tube and fission chamber). In this case, the performance of FE method isn't improved even when each assembly is divided into 4 nodes. As for computational time, since we treat each assembly as a node (only 9 nodes), the time for iteration decreases to a very small number in FE method. However, the time for computing response matrices increases rapidly with the expansion order. In FS method, the large number of vertices in the assembly causes the low efficiency in both response matrices generation and power iteration. Additionally, in practical cases, the thermal-hydraulic feedback and burnup effects are different everywhere in the core. Thus, every node is 'unique' and has its own cross sections which means we have to calculate the response matrices for each node. This would be very time consuming which makes it difficult to be employed in practical applications at present. Some acceleration schemes and improvements for this method is under study.

Violet-Het3D will be further improved to solve the neutron-transport equation in the future and it will be employed in more applications to improve the computational behavior of nodal methods by taking the advantage of directly treating heterogeneous nodes.

Acknowledgments

This work was financially supported by the National Natural Science Foundation of China (11305123).

References

Bandini, B.R., Aumiller, D.L., Tomlinson, E.T., 2003. An Algorithm to Correct for

Control Rod Cusping in NESTLE Multidimensional Neutronics Module of RELAP5-3D. Int. RELAP5-3D User Seminar, West Yellowstone, Montana, Aug. 27–29.

- D. Bernardi, F. Hecht, K. Ohtsuka, O. Pironneau, *freefem+* documentation, on the web at [ftp://www.freefem.org/freefemplus](http://www.freefem.org/freefemplus).
- Dall'Osso, A., 2002. Reducing Rod Cusping Effect in Nodal Expansion Method Calculation. Oct. 7–10. Proc. Physor, Seoul, Korea.
- Downar, T., Lee, D., Xu, Y., Kozlowski, T., 2004. Theory Manual for the PACKS Spatial Kinetics Core Simulator Module. School of Nuclear Engineering, Purdue University, West Lafayette, Indiana, USA.
- Fanning, T.H., Palmiotti, G., 1997. Variational nodal transport methods with heterogeneous nodes. Nucl. Sci. Eng. 127, 154–168.
- Han-Sem, Joo, 1984. Resolution of the Control Rod Cusping Problem for Nodal Methods. Ph.D. Thesis. Massachusetts Institute of Technology.
- Li, Y., Cao, L., Yuan, X., 2014a. High Order Source Approximation for the EFEN Method. Sept. 28–Oct. 3. Physor, Kyoto, Japan.
- Li, Y., Wang, Y., Wu, H., Cao, L., 2014b. Heterogeneous Variational Nodal Method with Continuous Cross Section Distribution in Space. ANS Winter Meeting, Anaheim, CA, USA, Nov. 9–13.
- Li, Y., Wang, Y., Liang, B., Shen, W., 2015a. Partitioned-matrix acceleration to the fission-source iteration of the variational nodal method. Prog. Nucl. Energy 85, 640–647.
- Li, Y., Wang, Y., Wu, H., Cao, L., 2015b. Heterogeneous Variational Nodal Methods for Eliminating the Control Rod Cusping Effect. ANS Winter Meeting, Washington D. C., USA, Nov. 8–12.
- Palmiotti, G., Lewis, E.E., Carrico, C.B., 1995. VARIANT: VARIational Anisotropic Nodal Transport for Multidimensional Cartesian and Hexagonal Geometry Calculation. ANL-95/40. Argonne National Laboratory, Argonne, IL USA.
- Reddy, J.N., 1993. An Introduction to the Finite Element Method. McGraw-Hill Education, Boston, Massachusetts, USA.
- Reitsma, F., Muller, E.Z., 2002. Flexible Exposure and Nodal Mesh Treatment in the 3D Nodal Simulator MGRAC: Application to a MTR Case with Axially Movable Assembly. Oct. 7–10. Physor, Seoul, Korea.
- Si, S.Y., 2006. Application of Control Rod Cusping Effect in Three Dimensional Reactor Core Nodal Code. Proc. Corphy, Haerbin, Heilongjiang.
- Smith, K.S., 1986. Assembly homogenization techniques for light water reactor analysis. Prog. Nucl. Energy 17 (3), 303–335.
- Smith, M.A., Tsoufanidis, N., Lewis, E.E., Palmiotti, G., Taiwo, T.A., 2003. A finite subelement generalization of the variational nodal method. Nucl. Sci. Eng. 144, 36–46.
- Tatsumi, M., Yamamoto, A., 2003. Advanced PWR core calculation based on multi-group nodal-transport method in three-dimensional pin-by-pin geometry. J. Nucl. Sci. Technol. 40 (6), 376–387.
- Yamamoto, A., 2004. A simple and efficient control rod cusping model for three-dimensional pin-by-pin core calculation. Jan. Nucl. Technol. 145.
- Yang, W., Zheng, Y., Wu, H., Cao, L., Li, Y., 2014. High-performance whole core pin-by-pin calculation based on EFEN-SP3 method. Nucl. Power Eng. (in Chin.) 35, 164–167.
- Zhang, T., 2014. Development of HEFT Code System for the Analysis of Highly Heterogeneous Research Reactors, 22, Prague, Czech Republic, Jul. 7–11. Proc. Icone.
- Zienkiewicz, O.C., Taylor, R.L., Zhu, J.Z., 2008. Finite Element Method: its Basis and Fundamentals, Beijing World Publishing Corporation. Beijing, China.